Accepted Manuscript

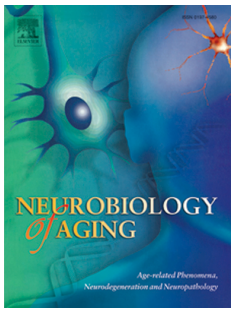

Enhanced Postsynaptic Inhibitory Strength In Hippocampcl Principal Cells In High Performing Aged Rats

Trinh Tran, Michela Gallagher, Alfredo Kirkwood

PII: S0197-4580(18)30212-4

DOI: 10.1016/j.neurobiolaging.2018.06.008

Reference: NBA 10280

To appear in: *Neurobiology of Aging*

Received Date: 11 April 2018

Revised Date: 28 May 2018

Accepted Date: 3 June 2018

Please cite this article as: Tran, T., Gallagher, M., Kirkwood, A., Enhanced Postsynaptic Inhibitory Strength In Hippocampcl Principal Cells In High Performing Aged Rats, *Neurobiology of Aging* (2018), doi: 10.1016/j.neurobiolaging.2018.06.008.

ENHANCED POSTSYNAPTIC INHIBITORY STRENGTH IN HIPPOCAMPCL PRINCIPAL CELLS IN HIGH PERFORMING AGED RATS

Trinh Tran[1], Michela Gallagher[2] and Alfredo Kirkwood[1]

1.Mind/Brain Institute and Department of Neurosciences,
2.Department of Psychological and Brain Sciences,
Johns Hopkins University,
3400 N. Charles St, Baltimore, MD 21218

Correspondence:
Michela Gallagher:
Department of Psychological and Brain Sciences
216B Ames Hall
3400 N. Charles St.
Baltimore, MD 21218
Phone: 410-516-0167
FAX: 410-516-6205
e-mail: michela@jhu.edu

Alfredo Kirkwood:
Mind Brain Institute
Johns Hopkins University
250 Dunning Hall
3400 N. Charles St.
Baltimore, MD 21218
Phone: 410-516-6410
FAX: 410-516-8648
e-mail: kirkwood@jhu.edu

Acknowledgments:. Supported by grant PO1-AG09973 from NIH.

ABSTRACT

Hyperactivity within the hippocampal formation, frequently observed in aged individuals, is thought to be a potential contributing mechanism to the memory decline often associated with aging. Consequently, we evaluated the postsynaptic strength of excitatory and inhibitory synapses in the granule cells of the dentate gyrus and CA1 pyramidal cells of a rat model of aging, in which each individual was behaviorally characterized as aged impaired (AI) or aged unimpaired (AU, with performance comparable to young (Y) individuals. In hippocampal slices of these 3 aged groups (Y, AI, AU) we found that, compared to the young, the miniature excitatory and inhibitory currents (mEPSCs and mIPSCs) were larger in amplitude in the granule cells of the AU group and smaller in the AI group. In contrast, in CA1 cells neither the mEPSCs nor the mIPSCs were affected by age, whereas the extrasynaptic conductance responsible for tonic inhibition was selectively enhanced in CA1 cells of AU individuals. Tonic inhibition conductance was not affected by age in the granule cells. These results support the notion that up-regulation of synaptic inhibition could be a necessary condition for the maintenance of performance during aging. These findings also underscore the notions that successful aging requires adaptive up-regulation, not merely the preservation of youthful functionality, and that age effects are not homogeneous across hippocampal subfields.

INTRODUCTION

Memory decline is a common but not inevitable consequence of aging. Individual differences in cognitive outcomes are observed in outbred aged rats, ranging from impairment in hippocampal-dependent memory to high performance on a par with young adults. Key findings on altered hippocampal function in this rodent model have translated to in vivo studies of humans with age-related memory decline (Leal and Yassa, 2015). That cross-species translation has centered on a loss of excitatory/inhibitory balance producing a condition of overactivity in hippocampal neural circuits that are critical for episodic memory. Alongside those findings, neurobiological studies of high-performing aged rats have shown engagement of neural mechanisms that differ not only from memory-impaired aged rats but also from young adults. Studies directed at the hippocampal formation have demonstrated that aged rats performing on a par young adult rats in a spatial memory task exhibit gene expression profiles, mechanisms for plasticity, and altered circuit/network function, which are distinct from younger rats, as well as from aged rats with impaired memory (e.g., (Yang et al.; Boric et al., 2008; Haberman et al.). Notably, evidence from such research has indicated a recruitment of inhibition in the aged rodent brain that could adaptively maintain a balance of excitation and inhibition required for intact memory. These findings on underlying individual differences associated with cognitive outcomes in aging prompted us to examine age-related alterations in excitatory and inhibitory synaptic transmission using in vitro hippocampal slices from behaviorally characterized rats.

Earlier studies have shown altered mechanisms for synaptic plasticity in the CA1 region according to cognitive outcomes in aging; in the aged CA1 region of the hippocampus NMDA-dependent synaptic plasticity is reduced in both memory- impaired and unimpaired individuals, but mGluR-dependent synaptic plasticity is augmented in the aged rats with preserved memory performance (Lee et al., 2005; Boric et al., 2008). Recent studies in both rodent and humans indicate that structural and functional alterations in the dentate gyrus (DG) region of the hippocampal formation are potential contributing mechanisms to the memory decline associated with aging (for review. see

Leal and Yassa, 2015). The corresponding mechanistic alterations within the synaptic circuitry of the aged DG, however, remain largely unknown.

Multiple lines of evidence support a role of the DG in the cognitive impairment associated with aging. Pattern separation, a key computational function for the encoding of new memories to ensure low interference with prior experience is widely thought to be subserved by DG. This computational function probed in memory performance that taxes pattern separation is diminished in memory impaired aged individuals (Leal and Yassa, 2018). Aged individuals with cognitive impairment, both rodents and humans, often exhibit an abnormally high level of neural excitability, particularly in the DG-CA3 region indicative of an imbalance in excitatory/inhibitory processes. A few studies have reported changes in excitatory and inhibitory synaptic transmission in the aged hippocampus, including the DG (Luebke and Rosene, 2003; Krause et al., 2008; Ardiles et al.; McQuail et al., 2015), but without evaluating their specific role in cognitive aging. Here, we focus on the excitatory and inhibitory properties of synaptic connections onto granule cells in the DG and the principal pyramidal neurons in the CA1 region of the hippocampus in a rat model in which aged animals are well characterized for cognitive status.

METHODS

Behavioral assessment.

Male Long-Evans outbred rats obtained pathogen-free from Charles River Laboratories (Raleigh, N.C.) were 6 month (young) or 24 month (aged) of age at the time of behavioral characterization for spatial learning in a water maze (1.83 m diameter, opaque water at 27˚C). During an eight-day period, in sessions consisting of three trials a day with a 60 s inter-trial interval, rats were trained to locate a camouflaged platform that remained in the same location 2 cm below the water surface. During a training trial, the rat was placed in the water at the perimeter of the pool and allowed 90 s to locate the escape platform. If at 90 s the rat failed to escape on a trial, it was placed onto the platform and allowed to remain there for 30 s. The position of entry for the animal was varied at each trial. Every sixth trial consisted of a free swim ("probe trial"), which served to assess the development of a spatially localized search for the escape platform. During probe trials the rat was allowed to swim a total of 30 s with the escape platform retracted to the bottom of the pool. After 30 s, the platform was raised so that the rat could complete escape on the trial. A "behavioral index", which was generated from the proximity of the rat to the escape platform during probe trial performance, was used in correlational analysis with the neurobiological data. This index is the sum of weighted proximity scores measured during probe trials; low scores reflect search near the escape platform whereas high scores reflect search farther away from the target. Thus, the "behavioral index" provides a measure that is based on search accuracy independent of escape velocity (Gallagher, 1993). "Search error" during training trials refers to the deviation from a direct path to the platform and provided an additional measure for behavioral analysis (Gallagher et al. 1993), Cue training (visible escape platform; 6 trials) occurred on the last day of training to test for sensorimotor and motivational factors independent of spatial learning. Rats that failed to meet a cue criterion of locating the visible platform within an averaged of 20 s over six trials were excluded from the experiments.

Electrophysiology

In all of these studies the experimenter was blind to the behavioral score of the subject. Behaviorally characterized young (6 months) and aged (24 months) rats were deeply anesthetized with isofluorane and under Urethane anesthesia (1g/Kg) were perfused transcardially with cold dissecting buffer (75 ml at 25 ml/min) containing 92 mM *N*-methyl-D-glucamine (NMDG), 2.5 mM KCl, 1.25 mM NaH_2PO_4, 30 mM $NaHCO_3$, 20 mM HEPES, 25 mM glucose, 2 mM thiourea, 5 mM Na-ascorbate, 3 mM Na-pyruvate, 0.5 mM $CaCl_2$ and 10 mM $MgSO_4$ pH adjusted to 7.4. After decapitation brains were removed quickly and coronal hippocampal slices (300μM) were made as described (Boric et al., 2008) in ice-cold dissection buffer bubbled with a mixture of 5% CO_2 and 95% O_2. The slices then recovered for 1 hr at room temperature in artificial cerebrospinal fluid (ACSF): 124 mM NaCl, 5 mM KCl, 1.25 mM NaH_2PO_4, 26 mM $NaHCO_3$, 10 mM dextrose, 1.5 mM $MgCl_2$, and 2.5 mM $CaCl_2$ bubbled with a mixture of 5% CO_2 and 95% O_2. The Institutional Animal Care and Use Committee at Johns Hopkins University approved all procedures

Visualized whole-cell voltage-clamp recordings. All recordings were done in a submerged recording chamber superfused with ACSF (30 ± 0.5°C, 2 ml/min). Visualized whole-cell voltage-clamp recordings were made from CA1 pyramidal cells or DG granule cells with glass pipettes (4-6 MOhms) filled with intracellular solution containing the following (in mM): 120 CsCl, 8 NaCl, 10 HEPES, 2 EGTA, 5 QX-314, 0.5 Na_2GTP, 4 MgATP, and 10 Na_2-phosphocreatine, pH adjusted to 7.25 with KOH, 280–290 mOsm. Membrane currents were recorded at -70 mV in the presence of 20 μM 6-cyano-7-nitroquinoxaline-2,3-dione (CNQX) and 100 μM 2-amino-5-phosphonovaleric acid (APV) and 0.5 μM Tetrodotoxin (TTX) to isolate miniature inhibitory postsynaptic currents (mIPSC), in the presence of 10 μM biccuculine methiodide (BMI) and 100 μM APV to isolate excitatory postsynaptic currents (mEPSC). We studied only cells with series resistance < 25 MΩ (17.6±0.3 MΩ in CA1; 20.1±1.0 MΩ in DG), an input resistance > 100 MΩ (151.5±2.7 MΩ in CA1; 524.7±41.7 MΩ in DG), and a RMS noise less than 3 in CA1 (2.20±0.04) and less than 4 in the DG (2.46±0.16) were studied. Membrane resistance and series resistance were monitored with 100-msec negative voltage commands (-4 mV) delivered every one minute. Cells were excluded if series resistance changed > 15% over the experiment. Data were

filtered at 2 kHz and digitized at 10 kHz using Igor Pro (WaveMetrics Inc., Lake Oswego, OR). All drugs were purchased from Sigma or R&D (Tocris).

Measurement of miniature excitatory and inhibitory postsynaptic currents (mEPSC and mIPSC). The amplitude and kinetic parameters of mEPSCs and mIPSCs were computed using the Mini Analysis Program (Synaptosoft) as previously described (Morales et al., 2002). For event discrimination we used an amplitude threshold of 3 times the RMS noise and a rise time<3 msec. The experimenter confirmed the events detected by the program. At least 100 events per cell were used in the calculations of mEPSCs, and 300 events for mIPSCs. The analysis focused on the shape and size of the events only because their frequency depends, besides the number of synapses, on multiple factors including ambient levels of neuromodulators that vary from slice to slice (Jeong et al., 2003; Goswami et al., 2012; Gao et al., 2017).

Measurement of maximal extrasynaptic GABAergic currents (tonic inhibition). Tonic currents were determined as described before (Huang et al., 2015) as the shift of baseline holding currents after the addition of $GABA_A$-receptor antagonist, BMI (20 μM) to the ACSF containing 5μM GABA, 20 μM CNQX and 100 μM APV. First, all-points histograms (bin width 2.5 pA) were generated for the control and bicuculline epochs (30 seconds). Then the histograms were fitted with a Gaussian model, and using only the left side of the distribution to avoid contamination with spontaneous event. The shift in the peaks of the Gaussian fits was used as the value for the tonic current (see Figure. 5A). To account for cell-to-cell size variability, the tonic currents were normalized to membrane capacitance (Cm), which was calculated from the integral of the transients of the test pulses. For brevity, we will refer the maximal normalized extrasynaptic GABAergic current available for tonic inhibition simply as “tonic inhibition”.

Statistical analysis. Statistical significance was determined with Prism GraphPad using ANOVA tests followed by Dunnet post hoc test when the data are distributed normally (judged by the D’Agostino-Pearson normality test), or by the Kruskal-Wallis (K-W) test followed by the Dunn test. Data distributions were compared with Kolmogorov-Smirnov (KS) test.

RESULTS

The central goal of the study was to determine changes in synaptic strength associated with cognitive aging in principal neurons across hippocampal subfields. To that end we, used whole-cell recordings to examine synaptic inputs in slices from young mature (6-month old) and aged (24-month old) outbred Long-Evans rats that had been behaviorally characterized in the water maze as described previously (see methods). Traditionally, whole-cell recordings have been restricted to slices from immature animals (typically less that 4-week old), but changes in the slice preparation described in methods enabled suitable visual and recordings conditions for visualized whole-cell clamp in mature and aged tissue, and with a yield (~4 cells/rat) comparable to what can be achieved in immature tissue (Gao et al., 2017). Altogether we recorded from 216 granule cells in the dentate gyrus of 52 rats and from 242 pyramidal cells in the CA1subfield of 66 rats. Recordings in aged CA3 are possible, but the yield is too low (about 1 cell/rat see (Simkin et al., 2015)) for the present study, which required correlating averaged measures of synaptic strength with the individual's performance.

Figure 1 summarizes the results for the behavioral assessment of the rats used in this study. Performance in the first trial (TT data point), before the rats had experienced escaping to the hidden platform in the water maze, was similar in both age groups. Over the course of training, however, young rats were more proficient in learning to locate the platform. A two-way ANOVA (Age x Trial Block) confirmed that performance improved over the course of training (Trial Block, $F(3,312) = 165.24$, $p = 0.0001$) but yielding a significant difference between age groups (Age, $F(1,312) = 70.05$, $p = 0.0001$). The interaction between Trial Block and Age was not significant, $F(3,312) = 1.089$, $p = 0.354$.The learning index scores (Fig. 1B), computed from a key measure of search accuracy during interleaved probe trials, also differed according to age ($t(169) = 6.43$; $p<0.0001$). In agreement with previous research in this model, the aged rats displayed a wide spectrum of outcomes, with many aged rats performing on par with young adults and a substantial group performing outside the range of young performance (Fig. 1B). Aged rats performing outside the range of the young group were designated aged impaired (AI), while those performing on par with young adults (Y) were designated

aged unimpaired (AU).

Enhanced postsynaptic strength of excitatory of synaptic transmission in granule cells of AU individuals.

We evaluated age-related changes in fast excitatory and inhibitory ionotropic transmission in granule cells by studying miniature events caused by spontaneous synaptic release (in the absence of action potentials). The amplitude of these miniature events (termed minis) provides a measure of postsynaptic strength that has been widely used in quantitative studies (Turrigiano et al., 1998; Kim and Tsien, 2008; Ardiles et al., 2012). The recordings were done in the cells located in the outer layer of either the upper or the lower blade of the dentate gyrus. The cells were readily visible and targetable for whole-cell recordings (Fig 2A, B).

First, we focused on miniature excitatory postsynaptic currents (mEPSCs) mediated by AMPARs, which were recorded in voltage clamp (Vh=-80mV) in the presence of 0.5 μM TTX, 100 μM APV and 10 μM BMI to block action potentials, NMDAR-mediated responses, and inhibitory responses, respectively. The results, summarized in Fig 2 and Table 1, indicate that the three groups did not differ either in the frequency of the mEPSCs (Table 1: p=0.3) or in the kinetic parameters of the isolated events (rise time: p=0.9; decay: p=0.8, Table 1, fig 2C, D). The only difference detected was in the amplitude of the events (Fig 2D-F; Table 1, p=0.02), which on average was significantly larger in cells recorded in the AU group that in the Y (Post hoc: p=0.04). We also examined the cumulative probability of the individual mEPSCs, and compared the distribution of these events for each of the groups. We found that, although the average mEPSCs amplitude of granule cells from AI rats was not significantly different on average from those recorded in AU and Y rats, the amplitude distribution of the individual events differed significantly (AI vs. Y: p=0.002; AI vs. AU: p=0.005. KS-test Fig 2F and Table 1). In the same vein, the amplitude distribution in AU was not simply a scaled-up version of the distribution in Y rats (AU scaled vs. Y: p=0.004. KS-test). Altogether, the results indicate a net increase in the strength excitatory synapses onto granule cells in AU rats, and also indicate that the effects of age are not homogenous across excitatory synapses based on differences in amplitude distributions as a function of age and cognitive phenotype.

The selective increase in the average mEPSC amplitude in the AU rats prompted us to examine whether this measure of synaptic strength was correlated with behavioral performance in aged rats. To that end, we computed the averaged mEPSC's amplitude from all the cells recorded in a given aged individual and plotted this value against the individual's behavioral performance in the Morris maze. Only individuals with 3 or more cells recorded were included in this analysis. As shown in Fig 2G, the individuals' mEPSCs amplitude including all aged subjects correlated significantly with behavioral performance such that elevated mEPSC amplitude was associated with better performance in spatial learning.

Postsynaptic strength of fast inhibitory synaptic transmission is larger in granule cells of AU individuals. The maintenance of a proper balance of excitation and inhibition is considered essential for neural processing. Previous studies suggest that aging can compromise the functional integrity of inhibitory circuits in the dentate gyrus (Spiegel et al., 2013; Koh et al., 2014) that are crucial for learning (Andrews-Zwilling et al., 2012). It was of great interest, therefore, to evaluate the effects of age on the postsynaptic strength of fast inhibitory transmission in granule cells of behaviorally characterized rats. We measured pharmacologically isolated miniature inhibitory postsynaptic currents (mIPSCs) using a similar experimental design as described above for mEPSC. The recordings were done at -80mV with electrodes filled with an internal solution based on CsCl and we blocked we blocked excitatory transmission by including 10 μM DNQX and 100 μM APV. As in the case of mEPSCs, we found that age significantly affected the IPSC amplitude, but not their kinetics (Fig 3A,B; Table 1). In contrast to the increase of mEPSCs, which affected only the AU group, the mIPSC amplitude was larger in the AU and reduced in the AI group (Fig 3C). A post hoc Dunnett test confirmed that each aged group (AI and AU) is different from the Y group. In a similar fashion, the distribution of the mIPSC differed among the 3 groups as confirmed by a KS-test (Y vs AU: $p=0.0007$; Y vs AI: $p<0.0001$: AU vs AI: $p<0.0001$. Fig 3D). Altogether, the results indicate that aging results in a net reduction in the strength of mIPSCs in impaired rats, and an increase in the AU rats.

As with the case of excitatory synapses, we also examined the relationship

between the averaged amplitude of the mIPSCs and the individual's behavioral score in the Morris maze. We plotted the averaged mIPSC's amplitude from all the cells recorded in a given aged individual (see methods) against the individual's performance score in the Morris maze spatial task. As shown in Fig 3D, we observed a significant correlation (R2, p=0.005) between the individual's mIPSC amplitude and behavioral performance such that lower mIPSC amplitude was associated with greater impairment.

Multiple types of inhibitory interneurons make contact with granule cells. Yet in juvenile mice, the relatively sparse CCK cells reportedly contribute the bulk of the IPSC because agonists of CB1 receptors (present in the terminals of CCK cells) dramatically reduce the mIPSC frequency (Goswami et al., 2012). We examined this possibility and found that this is not the case in mature individuals. Bath application of the CB1 agonist WIN (3 μM) did not affect the mIPSC frequency in either 4 month old Long Evans rats (104±4.5%, after 15 min in WIN, p=0.7; n=6 cells), or in 2 months old BL6 mice (104±4.5%, after WIN, p=0.7; n=6 cells. Data not shown).

Age does not affect the average postsynaptic strength of fast ionotropic transmission in CA1 pyramidal cells.

To complement the results obtained in the dentate gyrus, we also analyzed the effects of age on postsynaptic strength in the principal cells of the CA1 subfield behaviorally characterized young and aged rats. In these experiments, we recorded mEPSCs and mIPSCs in CA1 using the same methods as described above for granule cells. The conditions for recording, including visibility, were similarly adequate in the three aged groups, and the results for both types of events (mEPSCs and mIPSCs) are summarized in figure 4 and Table 2. Similar to the case of granule cells, we found that age has no significant effect on the kinetic parameters (time rise and decay) and the frequency of the mEPSCs (Fig 4 A,B, Table 3). In contrast with granule cells in the DG, however, the mEPSC amplitude in CA1 pyramidal cells also did not differ among the groups (Fig. 4C, Table 2). Consistent with that finding, there was no significant association of mEPSC amplitude averaged per individual and behavioral performance among the aged rats. Although the averaged mEPSCs were similar among the 3 age

groups, the distribution of the events in the aged groups and in the young group was different (AU vs. Y: p=0.004; AI vs. Y: p=0.00002; KS-test; Fig 4D) suggesting that age is associated with a redistribution of the postsynaptic weights within cells, but without impacting the average strength.

Next, we examined the status of inhibitory transmission, and quantified mIPSCs as a measure of postsynaptic strength. Similar to the case of mEPSCs reported above, we found no significant difference among the groups on the IPSCs in CA1 pyramidal cells (Fig 4F-J, Table 2). The mIPSCs were similar in their frequency (p=0,8) and kinetics (decay: p=0.9; rise time=0.8). Similar to the case of mEPSCs, the distribution of the individual IPSC amplitude differed across the aged and young groups (AI vs. Y: p<0.0001; KS=0.06565; AU vs. Y: p<0.0001; KS=0.08098), but the average mIPSC amplitude did not significantly differ (Table 2), suggesting that age redistributes postsynaptic weights without affecting the average strength of mIPSCs. Consistent with the absence of a net effect on amplitude, we also found no correlation between the amplitude of the mIPSCs averaged per individual and behavioral performance (Fig 4J). Altogether, the results indicate that age alone or differences in cognitive phenotype among the aged animals does not significantly alter the average postsynaptic strength of fast excitatory and inhibitory synaptic transmission in CA1 pyramidal cells.

Enhanced tonic inhibition in CA1 pyramidal cells from AU rats.

In the last set of studies we examined tonic inhibition in DG granule cells and CA1 pyramidal cells. Tonic inhibition is a slow current mediated by extrasynaptic $GABA_A$ receptors that have high affinity for GABA. These receptors can sense changes in ambient levels of GABA, and their activation increases the membrane conductance constraining cellular excitability (Lee and Maguire, 2014), dendritic integration (Groen et al., 2014), and the induction of synaptic plasticity (Smith, 2013; Groen et al., 2014). Importantly, in cortex tonic inhibition functionality is highly affected by age, experience and pathological conditions (Hines et al., 2012; Imbrosci et al., 2013; Huang et al., 2015; Carpenter et al., 2016); in hippocampus, age affects the expression of genes for $GABA_A$ subunits mediating tonic inhibition (Haberman et al., 2013).

We characterized tonic inhibition as the postsynaptic current induced by bath

application of saturating GABA as described in methods (Huang et al., 2015). At 5 μM GABA this concentration GABA maximally activates the extrasynaptic receptors responsible for tonic inhibition, but without affecting synaptic receptors involved in fast GABAergic transmission (Huang et al., 2015). In these conditions the change in the holding current after adding the $GABA_A$ blocker BMI (20μM) provides a direct estimate of the total tonic conductance available in a given cell (Fig. 5A). That current magnitude was then normalized by the cell's capacitance, a direct measure of the cell surface, to obtain a value that reflects the current density. This characterization of tonic inhibition has the advantage of being independent of the endogenous levels of extracellular GABA (Carver et al., 2016), which might vary from slice to slice.

The results are shown in figure 5B,C and Table 3. We found that in the dentate granule cells the value of tonic inhibition density did not differ significantly among the groups (KW=3.984; p = 0.14), although the values in the aged groups were slightly reduced numerically (Y=1.92±0.27pA/pF, n=21; AU=1.66±0.17pA/pF, n=17; AI=2.28±0.26 pA/pF, n=22). We also found that the average value of tonic inhibition in DG cells in aged individuals also did not correlate with the behavioral performance (r2=0.022; p=0.683). In contrast, in CA1 pyramidal cell's tonic inhibition was significantly larger in slices obtained from AU rats (Y=0.30±0.04 pA/pF, n=26; AU=0.62±0.06pA/pF, n=22; AI=0.46±0.09 pA/pF, n=23). Moreover, among aged rats the average value of tonic inhibition strongly correlated with the individual's performance in the Morris maze in CA1 pyramidal cells (Fig 5D). In sum, our results indicate that aging affects primarily tonic inhibition in CA1 and fast synaptic transmission in the dentate gyrus, in each case linked to the cognitive outcome represented by individual differences in hippocampal-dependent behavioral performance.

DISCUSSION.

The impact of aging on functional synaptic strength has been studied in a relatively small number of brain circuits (Foster et al., 1991; Sametsky et al., 2010; Hickmott and Dinse, 2013), but the association of any age-related changes with cognitive status has been rarely examined (Bories et al., 2013; Kumar and Foster, 2013; Luebke et al., 2015). The present comparison of the strength of ionotropic synaptic transmission in the granule cells of the dentate gyrus and CA1 pyramidal cells is the first performed in the hippocampus of behaviorally characterized aged rats. Our results indicate that in CA1 cells the magnitude of tonic inhibition is larger in aged unimpaired rats than in young rats, whereas in granule cells the amplitude of both mIPSCs and mEPSCs is larger in the aged unimpaired group, with mIPSCs significantly smaller in the impaired group. Additionally, the positive correlation between the strength of synaptic inhibition (tonic in CA1, mIPSCs in DG) and measures of learning in aged rats agrees with the emerging view that an excess of excitatory neural activity impairs learning in the aged brain (Haberman et al., 2017). These findings are also in line with the notion that the effects of aging vary across hippocampal subfields (Oh et al., 2016; Thome et al., 2016). Importantly, these data support the view that adaptive compensatory mechanisms rather than neurophysiology comparable to young adults contribute to the maintenance of cognition during aging (Lee et al., 2005; Boric et al., 2008; Haberman et al., 2013).

Our evaluation of the postsynaptic strength of inhibition revealed a selective reduction of the mIPSC amplitude in the granule cells of AI rats, which complements previous indications of an age-related dysfunction in the DG. Those studies reported a reduced content of the synthetizing enzyme GAD 67 in a subset of somatostatin (SOM) interneurons in the DG/hilus of AI individuals (Spiegel et al., 2013). The clear correlation between measures of both pre- and postsynaptic integrity on one hand, and the individual's behavioral performance on the other, is highly congruent with current views for an impact of aging in the dentate gyrus contributing to loss cognitive function. Strong GABAergic inhibition is essential for maintaining a sparse coding in the DG, i.e. very few cells firing at any given time, which in turn is crucial for the process of pattern separation during the encoding of new memories (Freund and Buzsaki, 1996; Acsady et

al., 2000; Houser, 2007; Myers and Scharfman, 2009). Consistent with that idea, hyperactivity within the dentate gyrus-DG/CA3 subregions is common in the AI individuals in this aging model (Wilson et al., 2003; Haberman et al., 2017), a condition that is also frequently observed in aged humans with impaired cognition and has also been identified in memory impaired non-human primates (e.g., (Yassa et al., 2011; Thome et al., 2016). Thus, we surmise that pre- and postsynaptic reductions in inhibitory drive likely contribute to hyperactivity and reduced performance in age-related memory impairment. In contrast, in aged individuals with preserved performance the average mIPSCs amplitude is larger than in young individuals, suggesting that increases in inhibitory drive can be adaptive.

The mechanisms underlying age-dependent changes in the IPSCs, and the identity of the parent interneurons of the affected synapses, remain to be determined. We ruled out that CCK interneurons, a relatively rare type that has been implicated in the bulk of the mIPSC's in juvenile granule cells, contribute to the IPSC's recorded in adults. The relative fast onset and decay of the mIPSC is consistent with synapses made by parvalbumin positive basket cells. Interestingly, the integrity of the synapses made by these cells appears to be compromised in humans affected by Alzheimer's disease (Xiao et al., 2017). As for mechanisms, it is worth noting that the IPSC's and the EPSC's are seemingly co-regulated; both are larger in the AU group and reduced in the AI group. This co-regulation of inhibition and excitation is reminiscent of homeostatic mechanisms that maintain the balance of excitation and inhibition in cortical circuits (Sprekeler, 2017).

Like the IPSC's, the postsynaptic strength of excitation (measured as EPSC average amplitude) also correlates with behavioral performance in the aged rats. Compared to the young group, the EPSC amplitude was larger in the AU group relative to the AI group. Those findings are congruent with a number of previous observations. In the Fisher 345 rat model of aging it was reported that the perforant path, which conveys excitatory inputs from the entorhinal cortex to granule cells, exhibits an age-dependent increase in the postsynaptic strength of unitary responses evoked by single axon stimulation (Foster et al., 1991). This increase in postsynaptic strength was interpreted to be a compensation for an age-dependent loss of perforant path axons, and

our present results suggest that this compensation might be restricted to an AU subpopulation with relatively preserved cognition. On the other hand, it seems plausible that the reduced EPSCs in the AI group represent synapses made by a population of neurons in the lateral entorhinal cortex identified to be particularly vulnerable to aging in rodents and humans (Smith et al., 2000; Stranahan et al., 2010; Yassa et al., 2010). This scenario of pre and post-synaptic deficits is consistent with the notion that in the long run mechanisms synaptic plasticity in the long run tend to match the strength of the pre- and postsynaptic partners (Lisman, 2017).

In contrast to granule cells, for CA1 pyramidal cells the numerically modest effects of age on mEPSCs and IPSCs amplitude did not reach significance, and the average amplitude of these synaptic events did not correlate with behavioral performance among the aged individuals. The absence of changes in the mEPSC amplitude is consistent with previous studies reporting no age-dependent changes in the field synaptic potentials (Lee et al., 2005) and in the spontaneous EPSC (Sametsky et al., 2010). On the other hand, and again in contrast to granule cells, in the CA1 pyramidal cells of aged rats tonic inhibition was larger in the unimpaired individuals, and it was the only synaptic conductance found to correlate with learning measures. This positive correlation again suggests an adaptive role for an larger tonic conductance during aging. In young adult rodents enhancing the recruitment of tonic inhibition and the concomitant reduction in excitability often impairs behavioral performance (Martin et al., 2010). Conditions are different in aged individuals, however, as CA1 cells face excessive neural input from CA3 (Wilson et al., 2003; Haberman et al., 2017). This excessive "neural noise" from CA3 could limit the efficacy of associative forms of synaptic plasticity that depend on detecting pre-and post-synaptic correlations. Thus, the age-related increase in CA1 tonic inhibition, by reducing somatic excitability and increasing the epsp-spike precision, might enhance the signal to noise ratio and improve memory encoding.

The mechanisms underlying the up-regulation of tonic inhibition in the aged unimpaired group remain to be determined. Our measurements were done under saturating ambient GABA, and under these conditions the larger conductance might reflect changes in unitary channel conductance or in the number of channels. In cortex changes in tonic conductance often correlate with altered expression of extrasynaptic

GABAR subunits. For example, in layer 2/3 pyramidal cells of sensory cortices, where tonic currents are carried primarily by GABARs containing the delta subunit, the expression of GABRAD and tonic conductance are both increased after ischemic insult (Imbrosci et al., 2013) and both decreased after sensory deprivation (Huang et al 2015). In CA1 and CA3 pyramidal cells tonic inhibition is primarily carried by receptors containing the alpha5 subunit (GABRA5). Previous studies detected a decrease in GABRA5 expression in the CA3 region of aged rats with impaired memory performance (Haberman et al., 2012). It seems plausible then that a larger GABRA5 expression and function in both CA1 and CA3 pyramidal cells is a necessary condition for optimal behavioral performance in aging, as expressed in this model.

The exact impact on hippocampal processing of the synaptic changes described here are difficult to evaluate because aging likely affects connectivity, intrinsic excitability as well as synapses in other neurons. Nevertheless, it must be noted that changes in mEPSC comparable to the ones reported here can profoundly affect sensory processing in cortex (Petrus et al., 2014), and comparable changes in mIPSC have been implicated in learning deficits in mouse models of neurological conditions (Chao et al., 2010; Sabanov et al., 2017). In addition, our finding that an enhanced postsynaptic strength of inhibition associates with youthful performance in the aged individuals is congruent with the emerging notion that hyperexcitability is a common and adverse consequence for aging. Of interest is the observation that different putative adaptive mechanisms operate in the two regions studied: larger tonic inhibition in CA1 and larger fast transmission in the DG. This raise the possibility that while hyperactivity might be prevalent across the aged brain, possible compensations need to be local.

FIGURE LEGENDS

Figure 1.Behavioral characterization of young (open circles) and aged rats (filled circles) in the Morris water maze. **A.** Cumulative search error measure of learning in five trial blocks during training. This measure reflects the distance of the rat from the escape platform throughout its search, with higher numbers indicating worse performance. Data points represent the average for blocks of five training trials ± SEM. Note that age groups do not differ on the first training trial (TT) but young rats are more proficient in learning to escape. **B.** A learning index measure for each rat was derived from proximity of the rat's search during probe trials (see methods and Gallagher et. al., 1993) with lower scores indicating more accurate performance. As a group aged rats exhibited significant impairment in accuracy, yet substantial variability. Approximately half of the aged rats performed more poorly than young rats (designated aged impaired), while a substantial subpopulation performed within the range of younger adults (designated aged unimpaired).

Figure 2. Larger amplitude of miniature EPSCs in granule cells of aged unimpaired rats. A, B) DIC pictures showing the granular layer of the DG in slices obtained from a young (A) and aged rat (B). Scale: 40 μm. On the right are amplified views of the indicated rectangle. (C, D) Example of current traces showing pharmacologically isolated mEPSCs recorded in granule cells from young (Y: green), aged unimpaired (AU: black), and aged impaired (AI: red) rats. D) Left: averages of all isolated events from all cells for each age group. Indicated on top is the number of cells. Right: the averaged traces were normalized by their amplitude and superimposed to reveal their similarity in the rise and decay kinetics. E) Average mEPSC amplitude per cell (circles) and the average ± s.e.m of displayed according to each age group. (F) The graph shows the distribution of the amplitudes of all mEPSCs recorded in the three age groups. G) Relationship between the behavioral score and the mEPSC magnitude averaged across cells in aged individuals. The line represents a linear fit of the data. * is $p<.05$ see Table 1 and text for additional details on the statistical analyses of these data.

Figure 3. Amplitude of miniature IPSCs is larger in granule cells of AU individuals and

smaller in AI individuals. A) Example traces showing pharmacologically isolated IPSC recorded in granule cells from young (Y: green), aged unimpaired (AU: black), and aged impaired (AI: red) rats. B) Left: averages of all isolated events from all cells for each age group. Indicated on top is the number of cells. Right: the averaged traces were normalized by their amplitude and superimposed to reveal their similarity in the rise and decay kinetics. C) Average mIPSC amplitude per cell (circles) and the average ± s.e.m of off cells displayed for each age group. D) The graph shows the amplitude distribution of all mEPSCs recorded in the three age groups. E) Relationship between the behavioral score and the mIPSC magnitude averaged across cells in aged individuals. The line represents a linear fit of the data. * $p < .05$ and see Table 1 and text for additional details on the statistical analyses of these data.

Figure 4. Aging does not affect the average amplitude of the mEPSCs and mIPSCs recorded in CA1 pyramidal cells. Panels on the left (A-I) display information about mEPSCs; panels on the right (B-J) display mIPSCs data. Top recordings are example traces showing pharmacologically isolated EPSCs (A) and mIPSCs (G) recorded in cells from young (Y: green), aged unimpaired (AU: black), and aged impaired (AI: red) rats. (B, F) Left: averages of all isolated events from all cells for each age group (mEPSCs on B; mIPSCs on F). Indicated on top is the number of cells. Right: the averaged traces were normalized by their amplitude and superimposed to reveal their similarity in the rise and decay kinetics. (C, H) Average event amplitude per cell (circles) and the average ± s.e.m of all cells displayed according to each age group. Data for mEPSC is shown in (C); mIPSC data shown in (H). (D, I) The graphs show the amplitude distribution of all events (mIPSCs or mEPSCs) recorded in the three age groups Data for mEPSCs on (D); mIPSC on (I). (I, J) Relationship between the behavioral score and the event magnitude averaged across cells in aged individuals. The line represents a linear fit of the data. Data for mEPSC in (I); mIPSC in (J). See detailed statistical analyses provided in Table 2

Figure 5. Enhanced tonic inhibition in CA1 pyramidal cells from AU rats. A) Experimental set-up. Holding currents were in the presence of (10 μM CNQX, 100 μM APV, 1 μM TTX, 5 μM GABA). Tonic inhibitory current (It) was determined as the

difference in the holding current measured before and after perfusion with 5 μM BMI. These values were normalized by the cell capacitance to obtain the current density. B-C) The graphs show the magnitude distribution of tonic inhibition (expressed as change in current density) recorded in cells from young (Y: green), aged unimpaired (AU: black), and aged impaired rats. Boxes represent the average ± s.e.m. In CA1 pyramidal cells (B) tonic inhibition is larger in the AU group, whereas in the dentate gyrus granule cells (C) there was no difference between the two age groups. D-E) Relationship between the behavioral score and tonic inhibition averaged across cells in aged individuals. The line represents a linear fit of the data. A clear correlation was detected for CA1 pyramidal (D), but not for DG granule cells (E). * $p<.05$ See Table 3 for statistical analyses.

Table 1

Recordings of mPSCs in granule cells

	mEPSCs				mIPSCs			
	Y (6, 19)	AU (8, 31)	AI (8,27)	P Stat	Y (5, 30)	AU (6, 29)	AI (6,33)	P Stat
Rise (ms)	1.77±0.03	1.78±0.03	1.79±0.02	0.9824 KW=0.036	1.32±0.04	1.28±0.04	1.34±0.03	0.4342 KW=0.036
Tau (ms)	5.29±0.10	4.88±0.16	4.93±0.15	0.0960 KW=4.69	10.5±0.43	10.7±0.31	9.96±0.31	0.1703 KW=3.54
Amp (pA)	14.3±0.43	**16.4±0.56***	14.9±0,50	0.017 $F_{2,74}$ 4.30	75.2±1.96	**82.4±2.71***	**67.36±1.68***	<0.0001 $F_{2,90}$ 12.80
Freq. (Hz)	1.29±0.14	2.03±0.32	1.68±025	0.6969 KW=0.722	1.63±0.15	1.33±0.08	1.43±012	0.0259 $F_{2,90}$ 3.810

Table 2

Recordings of mPSCs in pyramidal CA1 cells

	mEPSCs				mIPSCs			
	Y (6, 19)	AU (8, 31)	AI (7,27)	P Stat	Y (5, 30)	AU (6, 29)	AI (6,33)	P Stat
Rise (ms)	1.93±0.02	1.95±0.03	1.99±0.05	0.3133 KW=2.321	1.26±0.02	1.27±0.02	1.33±0.03	0.066 $F_{2,82}$ 2.88
Tau (ms)	5.46±0.17	5.76±0.23	5.52±0.21	0.0960 KW=4.69	9.52±0.20	9.58±0.23	10.2±0.34	0.1433 $F_{2,82}$ 1.99
Amp (pA)	22.6±1.03	20.3±0.84	20.64±0.96	0.297 KW=2.430	59.4±1.98	66.2±2.54	63.4±1.89	0.0943 $F_{2,82}$ 2.43
Freq. (Hz)	1.24±0.20	0.73±0.09	0.81±013	0.0500 KW=6.00	4.43±0.39	4.98±0.46	4.93±058	0.6931 $F_{2,82}$ 0.37

Table 3

Effects of age on the magnitude of tonic inhibition in granule and CA1 pyramidal cells

	Pyramidal cells in CA1				Granule cells in DG			
	Y (10, 26)	AU (6,22)	AI (8,23)	p stat	Y (5, 21)	AU (9, 17)	AI (8,22)	P Stat
It (pA/pF)	0.30±0.04	**0.62±0.06***	0.46±0.09	0.0039 F(2,68)=6.03	1.92±0.27	1.66±0.17	2.28±0.26	0.14 KW=3.984

REFERENCES

Acsady L, Katona I, Martinez-Guijarro FJ, Buzsaki G, Freund TF (2000) Unusual target selectivity of perisomatic inhibitory cells in the hilar region of the rat hippocampus. J Neurosci 20:6907-6919.

Andrews-Zwilling Y, Gillespie AK, Kravitz AV, Nelson AB, Devidze N, Lo I, Yoon SY, Bien-Ly N, Ring K, Zwilling D, Potter GB, Rubenstein JL, Kreitzer AC, Huang Y (2012) Hilar GABAergic interneuron activity controls spatial learning and memory retrieval. PLoS One 7:e40555.

Ardiles AO, Tapia-Rojas CC, Mandal M, Alexandre F, Kirkwood A, Inestrosa NC, Palacios AG (2012) Postsynaptic dysfunction is associated with spatial and object recognition memory loss in a natural model of Alzheimer's disease. Proc Natl Acad Sci U S A 109:13835-13840.

Boric K, Munoz P, Gallagher M, Kirkwood A (2008) Potential adaptive function for altered long-term potentiation mechanisms in aging hippocampus. J Neurosci 28:8034-8039.

Bories C, Husson Z, Guitton MJ, De Koninck Y (2013) Differential balance of prefrontal synaptic activity in successful versus unsuccessful cognitive aging. J Neurosci 33:1344-1356.

Carpenter HE, Kelly KB, Bizon JL, Frazier CJ (2016) Age-related changes in tonic activation of presynaptic versus extrasynaptic gamma-amniobutyric acid type B receptors in rat medial prefrontal cortex. Neurobiol Aging 45:88-97.

Carver CM, Chuang SH, Reddy DS (2016) Zinc Selectively Blocks Neurosteroid-Sensitive Extrasynaptic deltaGABAA Receptors in the Hippocampus. J Neurosci 36:8070-8077.

Chao HT, Chen H, Samaco RC, Xue M, Chahrour M, Yoo J, Neul JL, Gong S, Lu HC, Heintz N, Ekker M, Rubenstein JL, Noebels JL, Rosenmund C, Zoghbi HY (2010) Dysfunction in GABA signalling mediates autism-like stereotypies and Rett syndrome phenotypes. Nature 468:263-269.

Foster TC, Barnes CA, Rao G, McNaughton BL (1991) Increase in perforant path quantal size in aged F-344 rats. Neurobiol Aging 12:441-448.

Freund TF, Buzsaki G (1996) Interneurons of the hippocampus. Hippocampus 6:347-470.

Gallagher M (1993) Issues in the development of models for cognitive aging across primate and nonprimate species. Neurobiol Aging 14:631-633.

Gao M, Whitt JL, Huang S, Lee A, Mihalas S, Kirkwood A, Lee HK (2017) Experience-dependent homeostasis of 'noise' at inhibitory synapses preserves information coding in adult visual cortex. Philos Trans R Soc Lond B Biol Sci 372.

Goswami SP, Bucurenciu I, Jonas P (2012) Miniature IPSCs in hippocampal granule cells are triggered by voltage-gated Ca2+ channels via microdomain coupling. J Neurosci 32:14294-14304.

Groen MR, Paulsen O, Perez-Garci E, Nevian T, Wortel J, Dekker MP, Mansvelder HD, van Ooyen A, Meredith RM (2014) Development of dendritic tonic GABAergic

inhibition regulates excitability and plasticity in CA1 pyramidal neurons. J Neurophysiol 112:287-299.
Haberman RP, Quigley CK, Gallagher M (2012) Characterization of CpG island DNA methylation of impairment-related genes in a rat model of cognitive aging. Epigenetics 7:1008-1019.
Haberman RP, Koh MT, Gallagher M (2017) Heightened cortical excitability in aged rodents with memory impairment. Neurobiol Aging 54:144-151.
Haberman RP, Colantuoni C, Koh MT, Gallagher M (2013) Behaviorally activated mRNA expression profiles produce signatures of learning and enhanced inhibition in aged rats with preserved memory. PLoS One 8:e83674.
Hickmott P, Dinse H (2013) Effects of aging on properties of the local circuit in rat primary somatosensory cortex (S1) in vitro. Cereb Cortex 23:2500-2513.
Hines RM, Davies PA, Moss SJ, Maguire J (2012) Functional regulation of GABAA receptors in nervous system pathologies. Curr Opin Neurobiol 22:552-558.
Houser CR (2007) Interneurons of the dentate gyrus: an overview of cell types, terminal fields and neurochemical identity. Prog Brain Res 163:217-232.
Huang S, Hokenson K, Bandyopadhyay S, Russek SJ, Kirkwood A (2015) Brief Dark Exposure Reduces Tonic Inhibition in Visual Cortex. J Neurosci 35:15916-15920.
Imbrosci B, Neubacher U, White R, Eysel UT, Mittmann T (2013) Shift from phasic to tonic GABAergic transmission following laser-lesions in the rat visual cortex. Pflugers Arch 465:879-893.
Jeong HJ, Jang IS, Nabekura J, Akaike N (2003) Adenosine A1 receptor-mediated presynaptic inhibition of GABAergic transmission in immature rat hippocampal CA1 neurons. J Neurophysiol 89:1214-1222.
Kim J, Tsien RW (2008) Synapse-specific adaptations to inactivity in hippocampal circuits achieve homeostatic gain control while dampening network reverberation. Neuron 58:925-937.
Koh MT, Spiegel AM, Gallagher M (2014) Age-associated changes in hippocampal-dependent cognition in Diversity Outbred mice. Hippocampus 24:1300-1307.
Krause M, Yang Z, Rao G, Houston FP, Barnes CA (2008) Altered dendritic integration in hippocampal granule cells of spatial learning-impaired aged rats. J Neurophysiol 99:2769-2778.
Kumar A, Foster TC (2013) Linking redox regulation of NMDAR synaptic function to cognitive decline during aging. J Neurosci 33:15710-15715.
Leal SL, Yassa MA (2015) Neurocognitive Aging and the Hippocampus across Species. Trends Neurosci 38:800-812.
Lee HK, Min SS, Gallagher M, Kirkwood A (2005) NMDA receptor-independent long-term depression correlates with successful aging in rats. Nat Neurosci 8:1657-1659.
Lee V, Maguire J (2014) The impact of tonic GABAA receptor-mediated inhibition on neuronal excitability varies across brain region and cell type. Front Neural Circuits 8:3.
Lisman J (2017) Glutamatergic synapses are structurally and biochemically complex because of multiple plasticity processes: long-term potentiation, long-term

depression, short-term potentiation and scaling. Philos Trans R Soc Lond B Biol Sci 372.

Luebke JI, Rosene DL (2003) Aging alters dendritic morphology, input resistance, and inhibitory signaling in dentate granule cells of the rhesus monkey. J Comp Neurol 460:573-584.

Luebke JI, Medalla M, Amatrudo JM, Weaver CM, Crimins JL, Hunt B, Hof PR, Peters A (2015) Age-related changes to layer 3 pyramidal cells in the rhesus monkey visual cortex. Cereb Cortex 25:1454-1468.

Martin LJ, Zurek AA, MacDonald JF, Roder JC, Jackson MF, Orser BA (2010) Alpha5GABAA receptor activity sets the threshold for long-term potentiation and constrains hippocampus-dependent memory. J Neurosci 30:5269-5282.

McQuail JA, Frazier CJ, Bizon JL (2015) Molecular aspects of age-related cognitive decline: the role of GABA signaling. Trends Mol Med 21:450-460.

Morales B, Choi SY, Kirkwood A (2002) Dark rearing alters the development of GABAergic transmission in visual cortex. J Neurosci 22:8084-8090.

Myers CE, Scharfman HE (2009) A role for hilar cells in pattern separation in the dentate gyrus: a computational approach. Hippocampus 19:321-337.

Oh MM, Simkin D, Disterhoft JF (2016) Intrinsic Hippocampal Excitability Changes of Opposite Signs and Different Origins in CA1 and CA3 Pyramidal Neurons Underlie Aging-Related Cognitive Deficits. Front Syst Neurosci 10:52.

Petrus E, Isaiah A, Jones AP, Li D, Wang H, Lee HK, Kanold PO (2014) Crossmodal induction of thalamocortical potentiation leads to enhanced information processing in the auditory cortex. Neuron 81:664-673.

Sabanov V, Braat S, D'Andrea L, Willemsen R, Zeidler S, Rooms L, Bagni C, Kooy RF, Balschun D (2017) Impaired GABAergic inhibition in the hippocampus of Fmr1 knockout mice. Neuropharmacology 116:71-81.

Sametsky EA, Disterhoft JF, Geinisman Y, Nicholson DA (2010) Synaptic strength and postsynaptically silent synapses through advanced aging in rat hippocampal CA1 pyramidal neurons. Neurobiol Aging 31:813-825.

Simkin D, Hattori S, Ybarra N, Musial TF, Buss EW, Richter H, Oh MM, Nicholson DA, Disterhoft JF (2015) Aging-Related Hyperexcitability in CA3 Pyramidal Neurons Is Mediated by Enhanced A-Type K+ Channel Function and Expression. J Neurosci 35:13206-13218.

Smith SS (2013) alpha4betadelta GABAA receptors and tonic inhibitory current during adolescence: effects on mood and synaptic plasticity. Front Neural Circuits 7:135.

Smith TD, Adams MM, Gallagher M, Morrison JH, Rapp PR (2000) Circuit-specific alterations in hippocampal synaptophysin immunoreactivity predict spatial learning impairment in aged rats. J Neurosci 20:6587-6593.

Spiegel AM, Koh MT, Vogt NM, Rapp PR, Gallagher M (2013) Hilar interneuron vulnerability distinguishes aged rats with memory impairment. J Comp Neurol 521:3508-3523.

Sprekeler H (2017) Functional consequences of inhibitory plasticity: homeostasis, the excitation-inhibition balance and beyond. Curr Opin Neurobiol 43:198-203.

Stranahan AM, Haberman RP, Gallagher M (2010) Cognitive decline is associated with reduced reelin expression in the entorhinal cortex of aged rats. Cereb Cortex 21:392-400.

Thome A, Gray DT, Erickson CA, Lipa P, Barnes CA (2016) Memory impairment in aged primates is associated with region-specific network dysfunction. Mol Psychiatry 21:1257-1262.

Turrigiano GG, Leslie KR, Desai NS, Rutherford LC, Nelson SB (1998) Activity-dependent scaling of quantal amplitude in neocortical neurons. Nature 391:892-896.

Wilson IA, Ikonen S, McMahan RW, Gallagher M, Eichenbaum H, Tanila H (2003) Place cell rigidity correlates with impaired spatial learning in aged rats. Neurobiol Aging 24:297-305.

Xiao MF, Xu D, Craig MT, Pelkey KA, Chien CC, Shi Y, Zhang J, Resnick S, Pletnikova O, Salmon D, Brewer J, Edland S, Wegiel J, Tycko B, Savonenko A, Reeves RH, Troncoso JC, McBain CJ, Galasko D, Worley PF (2017) NPTX2 and cognitive dysfunction in Alzheimer's Disease. Elife 6.

Yang S, Megill A, Ardiles AO, Ransom S, Tran T, Koh MT, Lee HK, Gallagher M, Kirkwood A Integrity of mGluR-LTD in the associative/commissural inputs to CA3 correlates with successful aging in rats. J Neurosci 33:12670-12678.

Yassa MA, Muftuler LT, Stark CE (2010) Ultrahigh-resolution microstructural diffusion tensor imaging reveals perforant path degradation in aged humans in vivo. Proc Natl Acad Sci U S A 107:12687-12691.

Yassa MA, Lacy JW, Stark SM, Albert MS, Gallagher M, Stark CE (2011) Pattern separation deficits associated with increased hippocampal CA3 and dentate gyrus activity in nondemented older adults. Hippocampus 21:968-979.

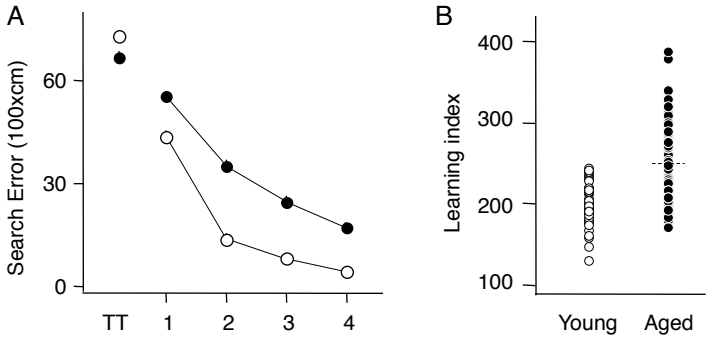

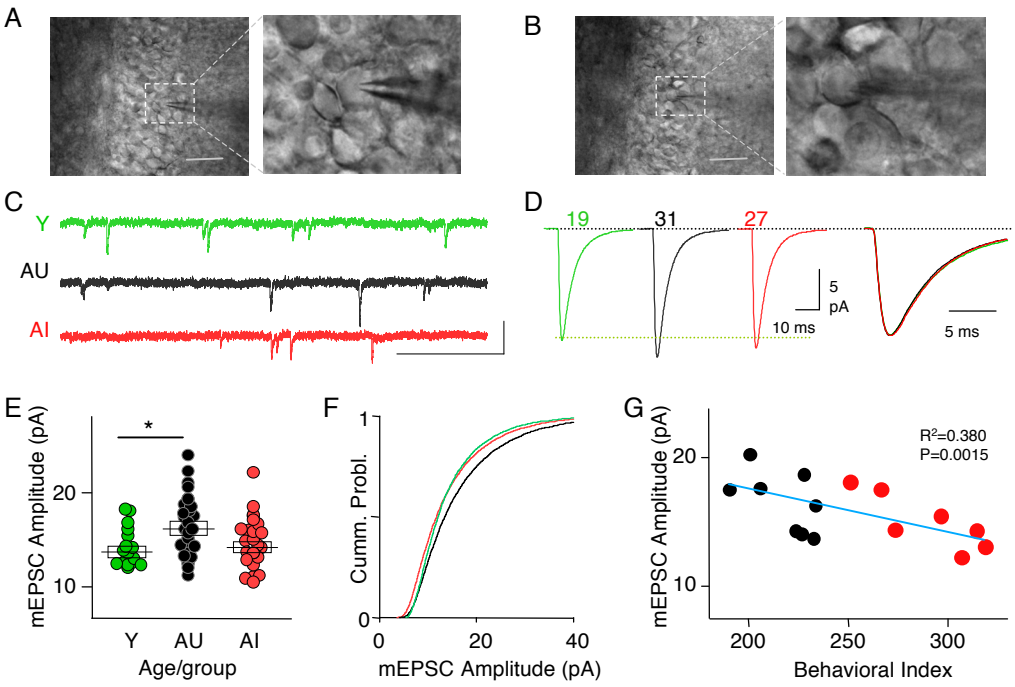
A
B
C
Y
AU
AI
D
19
31
27
5
pA
10 ms
5 ms
E
*
mEPSC Amplitude (pA)
20
10
Y
AU
AI
Age/group
F
Cumm. Probl.
1
0
0
20
40
mEPSC Amplitude (pA)
G
R²=0.380
P=0.0015
mEPSC Amplitude (pA)
20
10
200
250
300
Behavioral Index

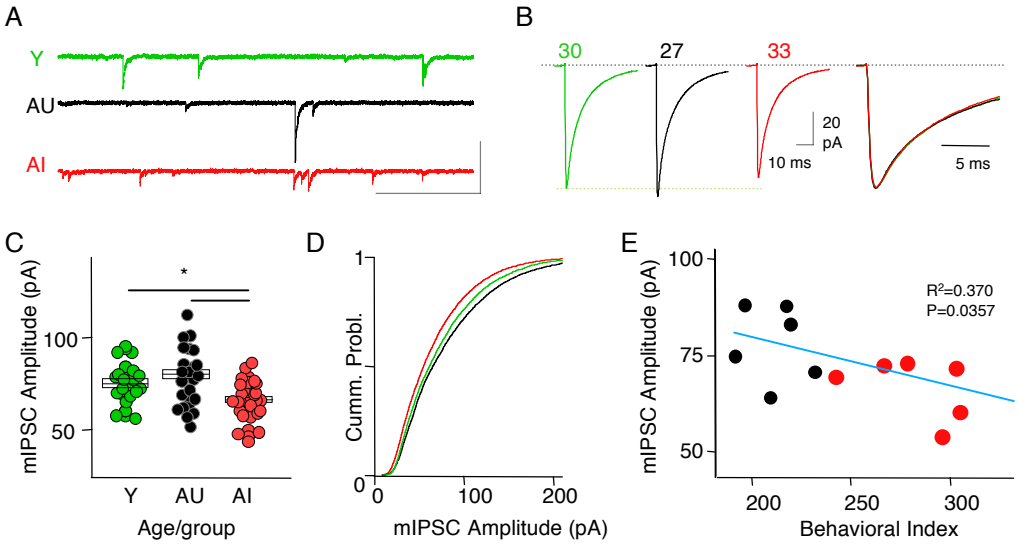
A
Y
AU
AI
B
30
27
33
20
pA
10 ms
5 ms
C
mIPSC Amplitude (pA)
100
50
*
Y
AU
AI
Age/group
D
Cumm. Probl.
1
0
0
100
200
mIPSC Amplitude (pA)
E
mIPSC Amplitude (pA)
100
75
50
R²=0.370
P=0.0357
200
250
300
Behavioral Index

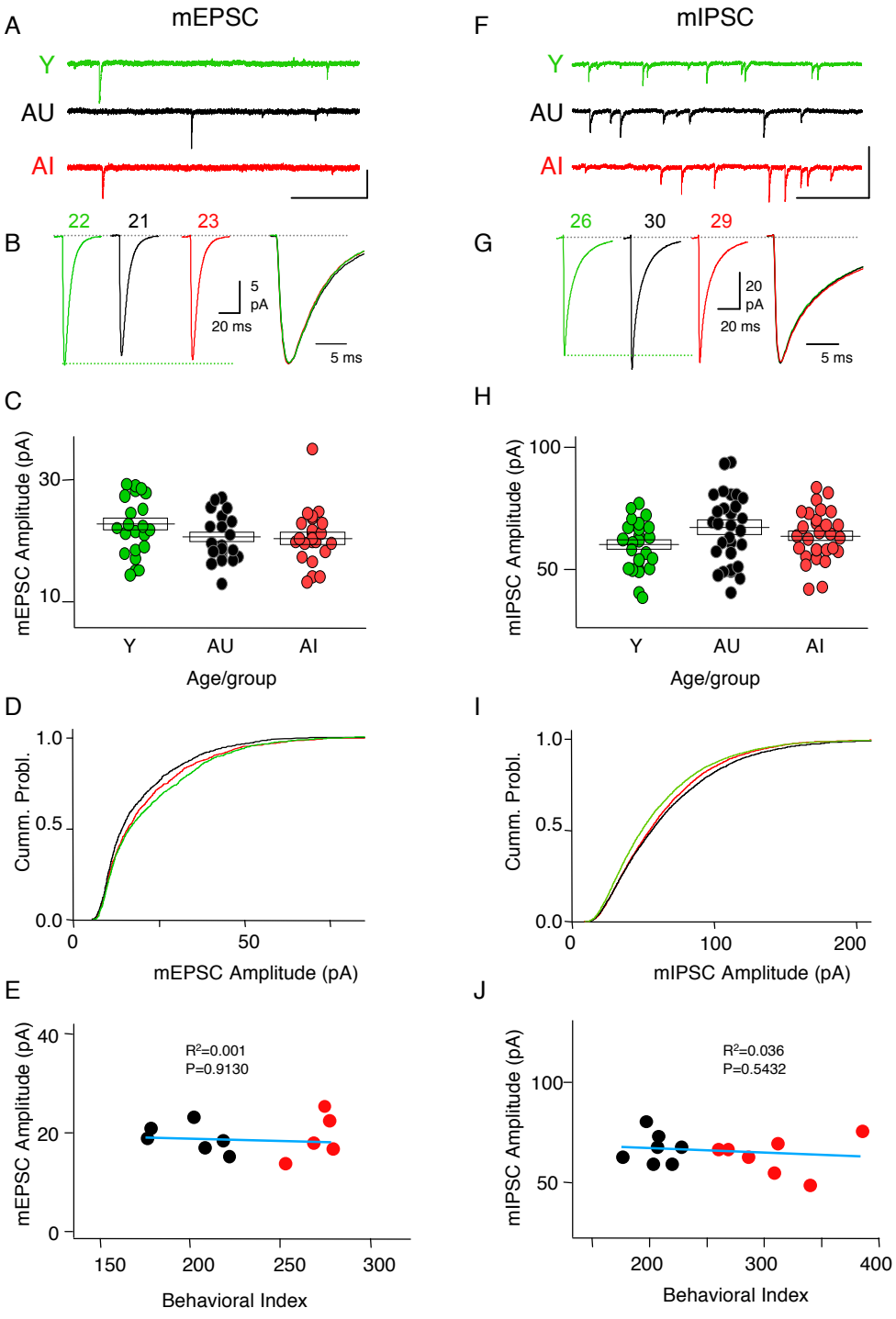
A
mEPSC
Y
AU
AI
B
22
21
23
5 pA
20 ms
5 ms
C
mEPSC Amplitude (pA)
30
10
Y
AU
AI
Age/group
D
Cumm. Probl.
1.0
0.5
0.0
0
50
mEPSC Amplitude (pA)
E
mEPSC Amplitude (pA)
40
20
0
R²=0.001
P=0.9130
150
200
250
300
Behavioral Index
F
mIPSC
Y
AU
AI
G
26
30
29
20 pA
20 ms
5 ms
H
mIPSC Amplitude (pA)
100
50
Y
AU
AI
Age/group
I
Cumm. Probl.
1.0
0.5
0.0
0
100
200
mIPSC Amplitude (pA)
J
mIPSC Amplitude (pA)
100
50
R²=0.036
P=0.5432
200
300
400
Behavioral Index

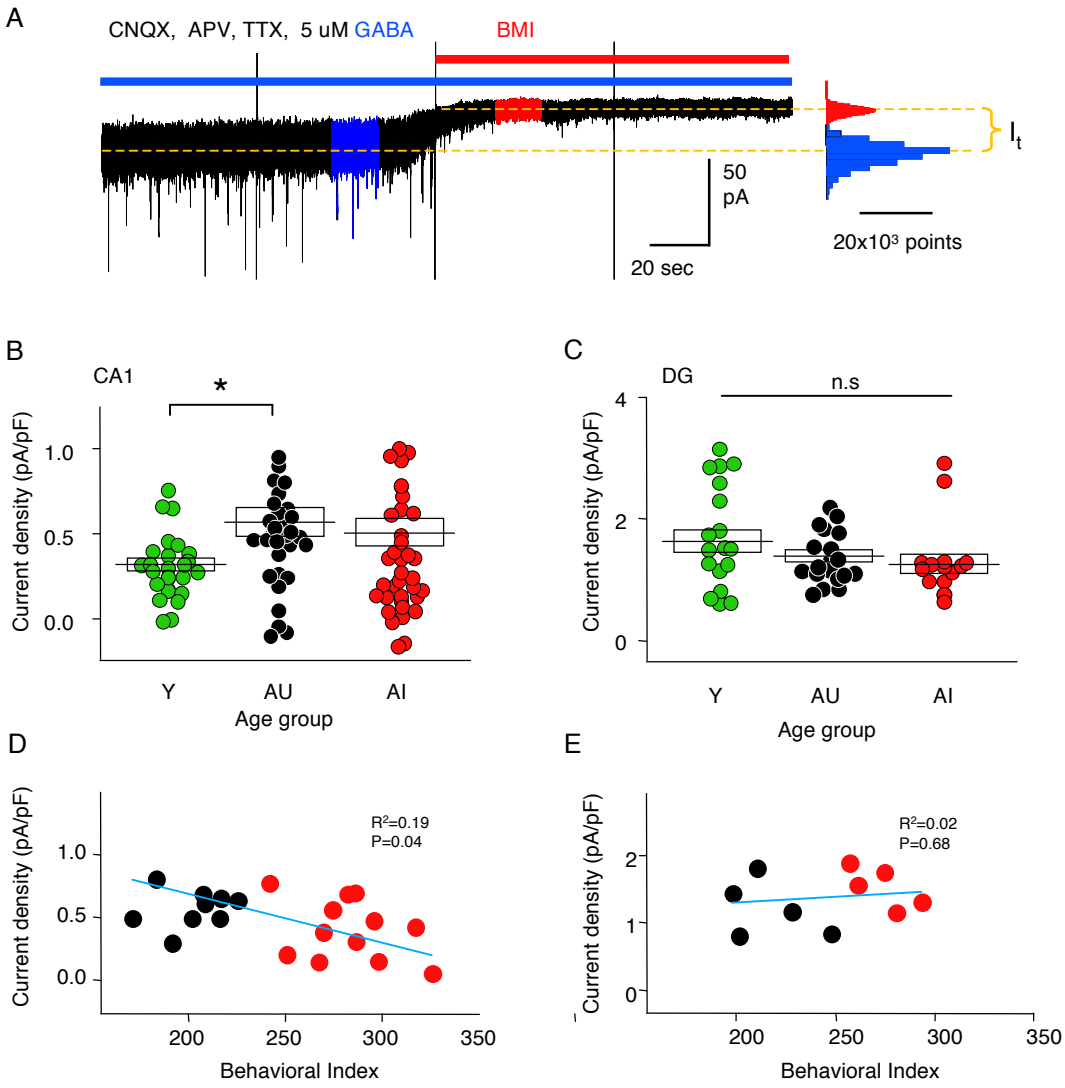
A
CNQX, APV, TTX, 5 uM GABA
BMI
I_t
50 pA
20 sec
20x10³ points
B
CA1
*
Current density (pA/pF)
1.0
0.5
0.0
Y
AU
AI
Age group
C
DG
n.s
4
2
0
Y
AU
AI
Age group
D
R^2=0.19
P=0.04
Current density (pA/pF)
1.0
0.5
0.0
200
250
300
350
Behavioral Index
E
R^2=0.02
P=0.68
Current density (pA/pF)
2
1
0
200
250
300
350
Behavioral Index